Complexation of Poly(vinyl alcohol)–Congo Red Aqueous Solutions. 2. SANS and SAXS Studies on Sol–Gel Transition

Mitsuhiro Shibayama,* Fumiyoshi Ikkai, and Shunji Nomura

Department of Polymer Science and Engineering, Kyoto Institute of Technology, Matsugasaki, Sakyo-ku, Kyoto 606, Japan

Received December 7, 1993; Revised Manuscript Received July 19, 1994®

ABSTRACT: Poly(vinyl alcohol)–congo red (PVA–CR) complexes in aqueous solutions undergo a reentrant sol–gel transition with respect to C_{CR} [Shibayama; et al. *Macromolecules* **1994**, *27*, 1738]. This transition was investigated from the structural viewpoints in terms of small angle neutron and X-ray scattering techniques. The static scattered intensity, $I(q)$, was observed as functions of PVA and CR concentrations, C_{PVA} and C_{CR}, and temperature, where q is the magnitude of the scattering vector. The contribution of the CR cluster scattering was successfully subtracted from $I(q)$, and the corrected scattered intensity function, $I_{corr}(q)$, was analyzed in terms of a so-called Kratky plot, i.e., $q^2I(q)$ vs q. A scattering maximum due to cluster formation and/or gelation was observed in the Kratky plot. $I_{corr}(q)$ was decomposed to Lorentz-type and Gauss-type scattering functions, where the Lorentz function represents the liquidlike fluctuations and the Gauss function indicates the presence of the static inhomogeneity created by complexation and/or gelation. The mechanism of the reentrant type sol–gel transition was discussed in terms of the structural parameters obtained by a curve fitting with this function.

Introduction

Polymer–ion complexes are formed by complexation between polymer chains and ions, mostly in an aqueous solution under a delicate balance among competing effects, i.e., complexation equilibria, polyelectrolyte effects, and reversible cross-linking. Because of a wide range of application, such as petroleum, food, photography, and cosmetics, polymer–ion complexes have attracted much attention in the past decades.[1–3] Poly(vinyl alcohol) (PVA) is one of the most popular polymers which is capable of ion complexation.[2–9] Particularly, PVA–borate complexes have been extensively studied by many workers. Sakurada applied the complex to PVA fiber manufacturing.[2] Recently, this technique was employed to prepare high-strength PVA fibers.[10] Ochiai et al.[4] studied the intrinsic viscosity behavior of PVA–borate ion complexes in aqueous solutions, which were theoretically explained by Leibler et al.[7] Sinton[6] and Shibayama et al.[8] studied the structure of the PVA–borate complexes with ^{11}B NMR. The sol–gel transition temperature of PVA–borate ion complexes was studied as functions of the degree of polymerization, polymer concentration, and cross-linker concentration.[9] Not only borate ions, but also several kinds of ions are known as cross-linkers for PVA gelation, such as cupric ions,[11] vanadate ions,[12,13] and Congo Red (CR).[14,15]

In the first paper of this series,[14] a viscosity behavior of PVA–CR ion complexes was investigated with a capillary viscometer. The reduced viscosity changed drastically by addition of CR to PVA solutions, which was interpreted by complexation equilibria and electrostatic screening effects. Then, a reentrant sol–gel transition was discussed from thermodynamic points of view. Figure 1 shows the sol–gel phase diagram for PVA–CR complexes in aqueous solutions. The solution was aged at 20 °C for 120 h after sample preparation. Open circles and open squares indicate that samples are in the sol and gel state, respectively. All the samples were clear in all concentrations studied here, implying that the systems were homogeneous and no phase demixing occurred in this concentration regime. The solid curve and the dashed line with C^*_{PVA} indicate the sol–gel phase boundary and the chain overlap concentration, respectively. C^*_{PVA} is estimated for the corresponding PVA aqueous solution in the unperturbed state.[14] It should be noted here that the phase diagram has a reentrant sol–gel transition behavior at C_{PVA} = 0.68 mol/L (30 g/L). This kind of sol–gel transition behavior was not found in PVA–borate ion complexes.[9,14–16] This is due to the fact that the ionic atmosphere of PVA–CR is very different from that of PVA–borate ion complexes. The PVA–CR ion complexes are formed around pH 7. This means that the electrostatic screening effect is much smaller than that of other systems such as PVA–borate ion complexes. It is also noteworthy that the reentrant sol–gel transition takes place exclusively near C^*_{PVA}.

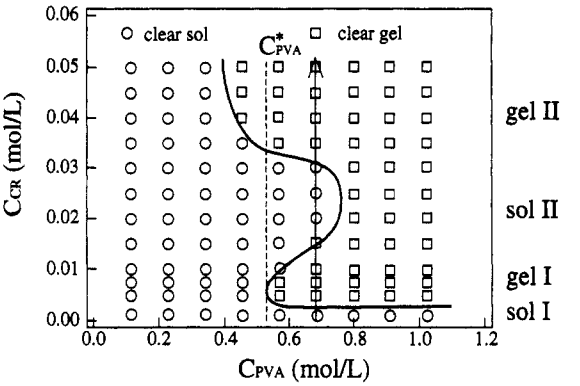

Figure 1. Sol–gel phase diagram of PVA–CR ion complexes. The open circles and squares indicate the state of the sample aged at 20 °C for 120 h. The solid curve indicates the sol–gel transition curve. All the samples were clear, and no demixing transition was observed. The dashed curve with C^*_{PVA} indicates the estimated chain overlap concentration. The arrow indicates the path where a reentrant sol–gel transition is observed.

Compared with a large number of rheological studies on polymer–ion complexes,[4,7–9,13–16] structure investigations on these systems have not been extensively studied.[17–19] In the case of chemically cross-linked polymer gels, small angle X-ray (SAXS) and/or neutron scattering (SANS) proved to be powerful tools to elucidate the microscopic view of the gel.[20–28] However, in the case of polymer–ion complexes, strong electrostatic interaction

* To whom correspondence should be addressed.

® Abstract published in *Advance ACS Abstracts*, September 1, 1994.

0024-9297/94/2227-6383$04.50/0

and reversible complexation make it difficult to develop a theoretical scattering function to account for these gels. We examine the scattered intensity function, $I(q)$, of the PVA–CR complexes so as to clarify the origin of the reentrant sol–gel transition behavior.

Theoretical Background

Structure factors for the gel, covering a wide range of the q space, have not been established yet. This is mainly due to the complexity of the cross-linking inhomogeneity introduced during the cross-linking process. Since a gel is a frozen system at least by the topological points of view, the structure factor of gels is greatly dependent on the method of preparation. A gel at a swelling equilibrium is described with an assembly of thermal blobs, which is the same as that of the corresponding polymer solution having the same concentration. Therefore, the scattered intensity, $I(q)$, of gels at $q \approx 1/\xi$ is given by[20,29]

$$I(q) = \frac{I(0)}{1 + \xi^2 q^2} \tag{1}$$

where ξ is the correlation length. However, for $q \ll 1/\xi$, $I(q)$ deviates from that for the corresponding polymer solution, as reported by Bastide et al.[20]

In order to take account of the static inhomogeneity created by cross-linking, Geissler and co-workers[21–25] decomposed $I(q)$ to Gauss-type and Lorentz-type structure factors, $I_G(q)$ and $I_L(q)$,

$$I(q) = I_G(q) + I_L(q) \tag{2}$$

$I_G(q)$ represents the static (frozen) inhomogeneity and is given by

$$I_G(q) = I_G(0) \exp\left[-\frac{\Xi^2 q^2}{3}\right] \tag{3}$$

where Ξ is the characteristic mean size of the static inhomogeneity.[25b] $I_L(q)$, on the other hand, represents liquidlike (dynamic) fluctuations and is given by

$$I_L(q) = \frac{I_L(0)}{1 + \xi^2 q^2} \tag{4}$$

where ξ is the correlation length. The net structure factor is then given by

$$I(q) = I_G(0) \exp\left[-\frac{\Xi^2 q^2}{3}\right] + \frac{I_L(0)}{1 + \xi^2 q^2} \tag{5}$$

Analyses of gel inhomogeneities using eq 5 were successfully conducted in several kinds of gels, particularly for nonionized gels (neutral gels), where observed scattered intensity functions were curve fitted with eq 5 and the structure parameters ξ and Ξ were estimated.[26–28]

Experimental Section

1. **Sample Preparation.** PVA powder with the degree of polymerization P = 1800 and the degree of saponification 99.96 mol % was dissolved in deionized hot water by stirring. After complete dissolution, the solution was mixed rigorously with an aqueous solution of reagent grade Congo Red and then gradually cooled to room temperature. For SANS experiments, deuterated water was used instead of deionized water. The details of the sample preparation were described elsewhere.[14]

2. **SAXS.** Small angle X-ray scattering (SAXS) experiments were performed at the Photon Factory of the National Laboratory for High Energy Physics, Tsukuba, Japan. The X-ray beam produced by synchrotron orbital radiation was monochromatized and collimated with a couple of Si(111) crystals and two sets of incident collimators. The wavelength of the incident beam was 1.488 Å. Samples were sealed in a stainless steel cell having a 5 μm thick polyester film window. The sample thickness was about 1 mm. The sample cell was mounted in a water-circulated temperature-controlled chamber. The scattered X-ray photons were counted with a one-dimensional position sensitive proportional counter, placed 1.9 m apart from the sample. The sampling time was 5 min each. The observed scattered intensity was corrected for absorption and cell scattering. The details of the equipment are described elsewhere.[30] Because of uncertainty of the sample thickness, the SAXS data were used only for qualitative discussion.

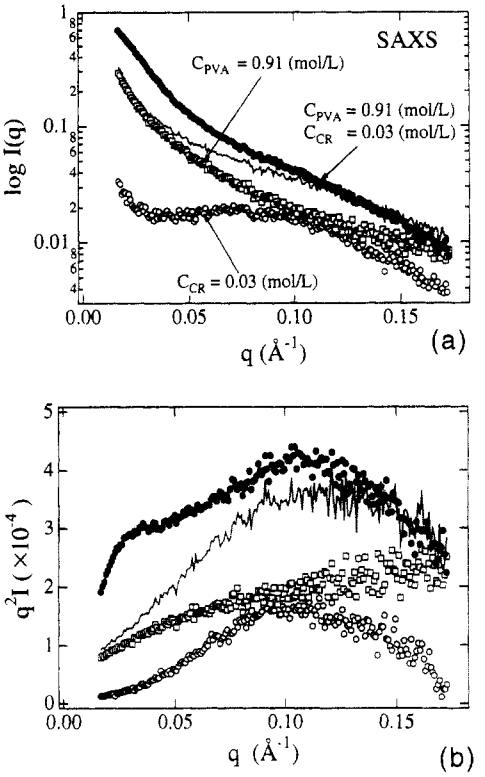

Figure 2. SAXS scattered intensity profiles of a CR aqueous solution, PVA aqueous solution, and PVA–CR ion complex gel: (a) linear plots; (b) Kratky plots.

3. **SANS.** Small angle neutron scattering (SANS) experiments were conducted at the research reactor, SANS-U, Institute of Solid State Physics, The University of Tokyo, which is located at the Japan Atomic Energy Research Institute, Tokai, Japan. Cold neutrons from the reactor were monochromatized with a velocity selector to a flux of neutrons, having the wavelength λ = 5 Å and the wavelength distribution $\Delta\lambda/\lambda$ = 0.1, which was used as the incident beam. Sample solutions were transferred into a quartz cell having optical path lengths of 1–4 mm. The observed scattered intensity was corrected for cell scattering and transmission and then rescaled to the absolute intensity with the incoherent scattering from a Lupolen standard[31] and with the elastic scattering from a blend film of deuterated and protonated PVA studied at the research reactor of the National Institute of Standards and Technology.[32]

Results

1. **Congo Red Scattering.** Figure 2a shows the SAXS scattered intensity profiles of a CR aqueous solution of C_{CR} = 0.03 mol/L, $I_{CR}(q)$, a PVA aqueous solution of C_{PVA} = 0.91 mol/L, $I_{PVA}(q)$, and a PVA–CR ion complex gel of C_{CR} = 0.03 mol/L and C_{PVA} = 0.91 mol/L, $I_{PVA/CR}(q)$. The dotted curve is the sum of $I_{PVA}(q)$ and $I_{CR}(q)$. As shown in the figure, CR has a broad peak maximum at q_m = 0.09 Å^{-1} whereas no peak maximum is detected for PVA. Note that ($=I_{PVA/CR}(q)$) cannot be expressed by the sum of

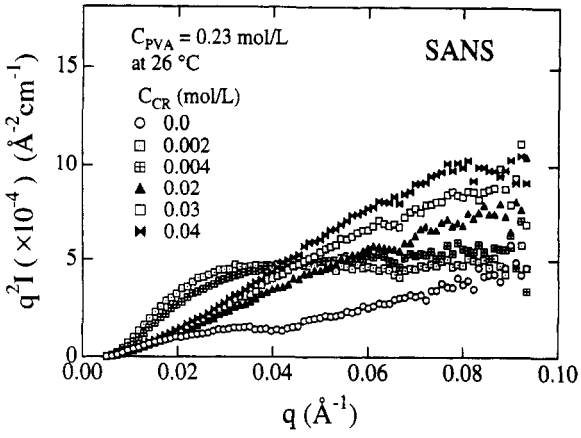

Figure 3. SANS Kratky plots for PVA–CR complexes of C_{PVA} = 0.23 mol/L at 26 °C.

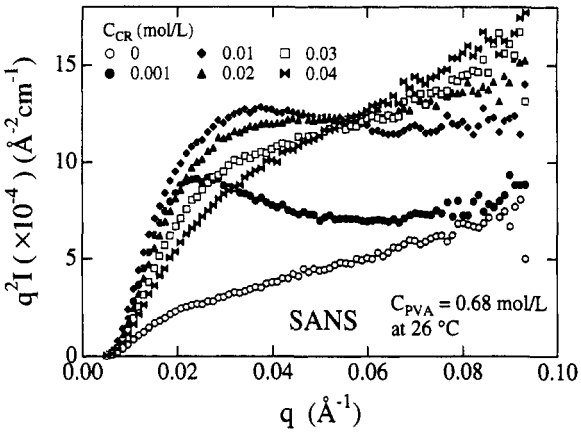

Figure 4. SANS Kratky plots for PVA–CR complexes of C_{PVA} = 0.68 mol/L at 26 °C.

$I_{PVA}(q)$ and $I_{CR}(q)$. This indicates a rearrangement of concentration fluctuations induced by complexation. For PVA–CR, $I(q)$ (=$I_{PVA/CR}(q)$) seems to have broad shoulders around 0.03 and 0.09 Å^{-1}. However, the presence of these shoulders is not clearly resolved.

Figure 2b is the so-called Kratky plot, i.e., a $q^2I(q)$ vs q plot, of the same sets of data. This figure clearly shows the presence of concentration fluctuations around 0.03 and 0.1 Å^{-1} for PVA–CR. The peak maximum at 0.1 Å^{-1} indicates CR ion clusters which are spaced about 60 Å (=$2\pi/q_m$). The other peak at 0.03 Å^{-1} is obviously due to the PVA–ion complexation in aqueous solutions. As shown in Figure 2b, the Kratky plot seems to be a relevant way to examine a modulation of the structure factor from that for a neutral polymer solution. Thus we discuss the scattered intensity functions with a Kratky plot.

2. Concentration Dependence. Figure 3 shows the SANS Kratky plots for C_{PVA} = 0.23 mol/L having several Congo Red concentrations at 26 °C. All the samples were in the sol state, as shown in Figure 1. For C_{CR} = 0.0 mol/L, $q^2I(q)$ is a monotonous increasing function of q. However, an addition of a small amount of CR, such as 0.002 and 0.004 mol/L, leads to creation of a hump at around q = 0.03 Å^{-1}. This hump gradually disappeared upon further addition of CR.

Figure 4 shows the SANS Kratky plots for C_{PVA} = 0.68 mol/L having several Congo Red concentrations at 26 °C. When C_{CR} = 0 mol/L, the $q^2I(q)$ curve gradually increases with q. However, by adding only 0.001 mol/L of CR, it starts to have a peak at 0.02 Å^{-1}. This peak grows and moves to q_m = 0.03 Å^{-1} by further addition of CR up to C_{CR} = 0.01 mol/L and then gradually decreases with C_{CR}. The appearance of this peak indicates formation of static

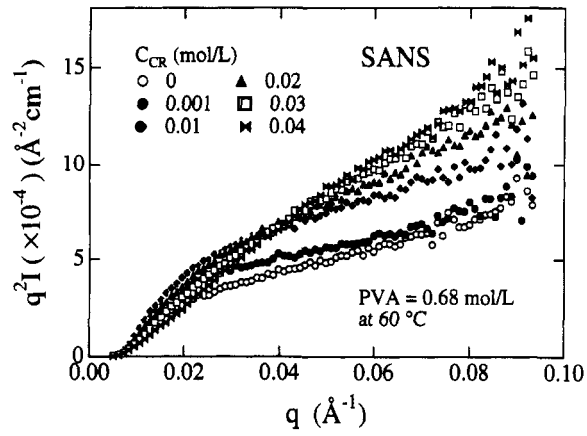

Figure 5. SANS Kratky plots for PVA–CR complexes of C_{PVA} = 0.68 mol/L at 60 °C.

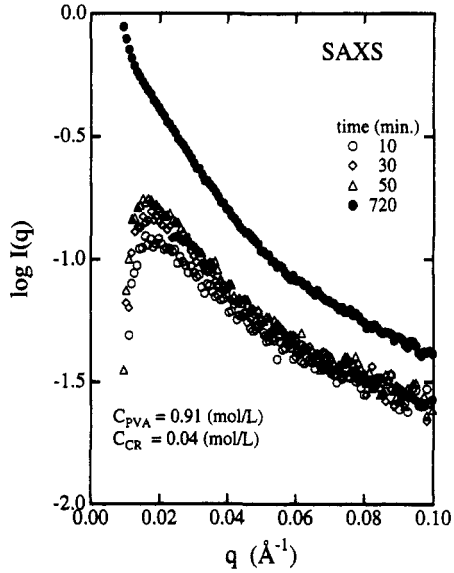

Figure 6. Time evolution of the SAXS intensity profiles for C_{PVA} = 0.91 mol/L and C_{CR} = 0.04 mol/L at 26 °C.

inhomogeneity due to complexation between PVA chains and CR ions. The upturn at higher q for $C_{CR} \geq 0.03$ mol/L is due to the scattering of CR clusters, having the scattering maximum at q_m = 0.1 Å^{-1}, as shown in Figure 2b.

3. Temperature Dependence. When the temperature was increased above the sol–gel transition, a homogeneous solution of sol was obtained. As was confirmed in the previous paper,[14] PVA–CR complexes become a sol at 60 °C, irrespective of PVA and CR concentrations. Figure 5 shows the SANS Kratky plots for C_{PVA} = 0.68 mol/L having several Congo Red concentrations at 60 °C. By comparing with Figure 4, it is obvious that the peak observed at 0.03 Å^{-1} in Figure 4 is greatly suppressed by temperature elevation up to 60 °C. Thus, the change of the structure factors upon a temperature change is clearly resolved by the Kratky plot. The gradual increase in $q^2I(q)$ with q results again from the CR cluster scattering.

4. Time Dependence. In the preceding sections, we have not discussed the time course of complexation, although it was noted that the phase diagram in Figure 1 was obtained by aging for 120 h. Here we briefly discuss the time dependence of the complexation.

Figure 6 shows time evolution of the SAXS intensity profiles for C_{PVA} = 0.91 mol/L and C_{CR} = 0.04 mol/L at 26 °C quenched from 60 °C. The experiment was conducted every 10 min up to 60 min. Experiments for longer aging times were not conducted because of the limitation of the beam time. The SAXS profile after 720

Table 1. Contrast Factors of CR/Water and PVA/Water for SANS and SAXS[a]

i/j	SANS K_{ij}^N (cm^{-1})	SAXS K_{ij}^X (mol electrons^2/cm^6)
CR/water	0.021	0.022
PVA/water	0.095	0.017

[a] The following mass densities were used for the calculation of the contrast factors: PVA, 1.26 g/cm^3 (amorphous density), CR, 1.62 g/cm^3 (measured by pycnometry).

min (12 h) is indicated with closed circles. This shows that the complexation process lasts on the order of hours, which is again in accord with the time evolution of the reduced viscosity for PVA–CR complex solutions in the dilute regime.[14]

Discussions

Based on the experimental evidence shown above, we discuss the structure factor of the PVA–CR ion complexes in aqueous solutions in detail. One should bear in mind the following facts: (1) The PVA–CR ion complex solution is a ternary system consisting of PVA, CR, and water. (2) The structure factor of PVA chains is strongly modulated due to the ion complexation and cross-link formation (gelation and/or clustering).

1. Contrast Factor. The contrast factors of neutron and X-ray scattering, K_{ij}^N and K_{ij}^X, respectively, are given by

$$K_{ij}^N = N_A v_j \left(\frac{a_i}{v_i} - \frac{a_j}{v_j}\right)^2 \quad (6)$$

$$K_{ij}^X = (\rho_i^e - \rho_j^e)^2 \quad (7)$$

where N_A is Avogadro's number and a_k, v_k, and ρ_k^e are the scattering length, the molar volume, and the electron density of the k (=i or j) component, respectively. Table 1 shows the contrast factors of neutron and X-ray scattering for CR/water and PVA/water. In the case of X-ray scattering, K_{CS} ($\equiv K_{CS}^X$) is larger than K_{PS} ($\equiv K_{PS}^X$) by a factor of 1.3. Therefore the contribution of CR scattering to the net scattering is about 30% larger that of PVA. In the case of SANS, on the other hand, K_{PS}^N is about 4.3 times as large as K_{CS}^N, indicating PVA scattering is much stronger than CR scattering. Thus it is clear that the inhomogeneity of the PVA–CR complexes due to rearrangement of PVA chains is detected much better by SANS than by SAXS.

2. Subtraction of the CR Cluster Scattering. The scattered intensity function for a ternary system composed of PVA, CR, and solvent is given by

$$I(q) = \phi_P\phi_C K_{PC} S_{PC}(q) + \phi_P\phi_S K_{PS} S_{PS}(q) + \phi_C\phi_S K_{CS} S_{CS}(q) \quad (8)$$

where $S_{ij}(q)$ is the structure factor between i and j. P, C, and S denote the polymer (PVA), cross-linker (CR), and solvent (water), respectively. K_{ij} usually depends on the geometry and the kinds of radiation (X-ray or neutron) unless $I(q)$ is rescaled to the absolute intensity. In the case of $\phi_P \ll 1$ and $\phi_C \ll 1$, the first term of the right hand side in eq 8 can be neglected. Thus,

$$I(q) \cong \phi_P\phi_S K_{PS} S_{PS}(q) + \phi_C\phi_S K_{CS} S_{CS}(q) = I_{PS}(q) + I_{CS}(q) \quad (9)$$

If the two kind of solutes, i.e., P and C, do not interact with each other, $S_{ij}(q)$ can be replaced by $S^\circ_{ij}(q)$, the structure factor of P (or C) in the solvent S without C (or P). Since the estimated contrast factors in Table 1 were not precise enough to directly estimate $S_{CS}(q)$ from the SAXS and SANS results, we assumed that $S_{CS}(q)$, the structure factor for CR/water in a PVA/CR/water ternary system, was the same as $S^\circ_{CS}(q)$, the structure factor for CR/water in a CR/water binary system. Thus we evaluated the polymer–solvent structure factor, $I_{PS}(q)$, by subtracting $I_{CS}(q)$ from $I(q)$,

$$I_{corr}(q) \equiv I_{PS}(q) = I(q) - I_{CS}(q) \quad (10)$$

This assumption may not be valid when C_{CR} is low since a significant redistribution of PVA chains as well as CR ions may occur due to complexation. However, for high C_{CR}'s, free CR ions exceed PVA-chain-bound ions and the free ions shield electrostatic interactions between bound ions, which results in recovering a neutral chain behavior of PVA chains. Therefore scattering from free CR ions can be easily removed by subtraction.

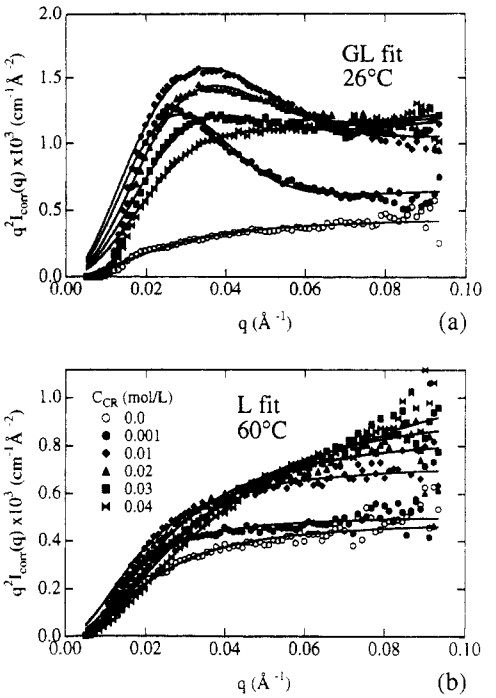

Figure 7. SANS Kratky plots of the corrected scattered intensity, $I_{corr}(q)$, for PVA–CR complexes of C_{PVA} = 0.68 mol/L at (a) 26 °C and at (b) 60 °C. The solid curves are the fitted curves with the Gauss–Lorentz function (GL fit) or with the Lorentz function (L fit).

3. Quantitative Analysis of the Structure Factor. Figure 7 shows the Kratky plots of the corrected scattered intensity, $I_{corr}(q)$, for C_{PVA} = 0.68 mol/L, having several CR concentrations at (a) 26 °C and (b) 60 °C. Compared with Figures 4 and 5, it is clear that the contribution of the CR scattering is effectively removed. Figure 7a clearly discriminates the samples with strong static inhomogeneities (C_{CR} = 0.001, 0.01, and 0.02 mol/L) from others (C_{CR} = 0.0, 0.03, and 0.04 mol/L) by the appearance of the peak at 0.02–0.04 Å^{-1}.

The solid curves in Figure 7a denote the reconstructed scattered intensity functions with eq 5, i.e., the Gauss–Lorentz (GL) type function. The fitting region was 0.016–0.081 Å^{-1}. However, for the cases of C_{CR} = 0.0 mol/L at 26 °C and all at 60 °C, the curve fitting was conducted by using only the Lorentz component, $I_L(q)$, since the system was in the sol state (L fit). As shown in the figures, all the

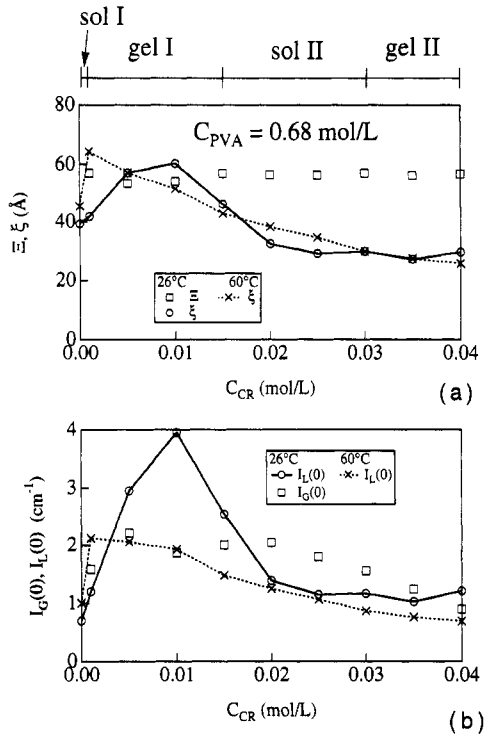

Figure 8. Variation of the structure parameters obtained with the GL or L fit: (a) Ξ and ξ; (b) $I_G(0)$ and $I_L(0)$. The scale on the top indicates the state of the system at 26 °C.

observed scattered intensity curves are well reproduced with the fitted ones.

Figure 8 shows the variation of the structure parameters of (a) Ξ and ξ and of (b) $I_G(0)$ and $I_L(0)$ as a function of C_{CR} for PVA–CR complexes of C_{PVA} = 0.68 mol/L. The solid and dashed curves indicate the values of ξ taken at 26 and 60 °C, respectively. The scale on the top of the figure indicates the state of the system at 26 °C. It should be noted here that the state of the sample, i.e., sol or gel, was observed by the flow behavior of the sample and thus it does not necessarily agree to the change of the microscopic structures. Theoretically, the gelation is characterized as a formation of an infinite cluster and is observed as the lack of flow.[33] On the other hand, the scattering cannot distinguish the infinite clusters from finite clusters near the gelation threshold. Furthermore, it is known that the sol–gel transition of a thermoreversible gel is rather smooth (not discrete) and it is difficult to determine precisely the transition temperature. It is obvious that even in the samples at C_{CR} = 0.02 and 0.03 mol/L ("sol" from the phase behavior), PVA chains are heavily complexed with CR ions. Thus the GL-type function fitting was employed even though those samples flowed ("sol").

Although ξ at 60 °C decreases gradually with C_{CR}, ξ at 26 °C increases in the limited region where gelation was observed (gel I) and then decreases with C_{CR}. The region where ξ at 26 °C is smaller than ξ at 60 °C is in accordance with the sol II region. The decrease in ξ at 60 °C with C_{CR} corresponds to the increase of the electrostatic screening effect with C_{CR}. The positive and negative deviations of ξ at 26 °C from ξ at 60 °C may indicate the chain expansion due to monocomplexation (ionization of PVA chains) and chain contraction due to intramolecular cross-linking, respectively. This is supported by the experimental evidence on the C_{CR} dependence of the reduced viscosity.[14,15] Ξ, on the contrary, does not depend strongly on C_{CR}.

Regarding Figure 8b, we expect an increase of $I_G(0)$ and a decrease of $I_L(0)$ in a gel state since the static inhomogeneity is significant in the gel region. However, the variations of the estimated $I_G(0)$ and $I_L(0)$ are different from our expectation. This may be explained as follows: The Gaussian component is inevitable to reproduce the observed scattered intensity function from a system having concentration fluctuations by complexation and/or gelation. However, it is verified by a simulation that $I_G(0)$ is not necessary to be larger than $I_L(0)$ to represent such fluctuations. For example, only 20% addition of the Gaussian component gives rise to a definite scattering maximum in the Kratky plot.[34] However this is the case when Ξ is equal to ξ. When either Ξ or ξ changes, the criterion of a peak appearance in the Kratky plot in terms of the relative magnitude of $I_G(0)$ and $I_L(0)$ is no longer valid. The apparent increase in $I_L(0)$ in the gel I region is due to the significant increase in ξ, since it affects $I_L(0)$ with the following relation:[29]

$$I_L(0) \sim C_{PVA}^2 E^{-1} \sim \Pi^{-1} \sim \xi^3 \qquad (11)$$

where E and Π are the bulk modulus and the osmotic pressure of the system, respectively. Thus the variation of the structure parameters indicates the change of the phase from sol I to gel I (appearance of the Gauss component) and gel I to sol II. However these parameters do not seem to be sensitive to the successive transition from sol II to gel II. This may be due to a strong screening effect of CR ions.

4. Reentrant Phase Behavior. On the basis of the facts disclosed in the preceding section, the reentrant sol–gel transition seen in Figure 1 is explained as follows: The first sol-to-gel transition occurs by chain expansion, which is initiated by monocomplexation of CR ions to PVA chains. This lowers C^*_{PVA} and leads to another complexation, i.e., dicomplexation, to another PVA chain. Cross-links are thus formed (gel I). By increasing C_{CR}, electrorepulsive interaction becomes dominant, resulting in gel melting (sol II). A further increase of C_{CR} suppresses the repulsive interaction, and dicomplexation (cross-link formation) is recovered (gel II). This kind of sol–gel transition is on a delicate balance among monocomplexation, dicomplexation, and the electrostatic screening effect. In addition, the transition requires a polymer concentration close to the chain overlap concentration, C^*. This explanation is consistent with the results obtained by the thermodynamic considerations of gel melting[14] and the capillary viscosity measurement.[15]

Concluding Remarks

The structure factors of PVA–CR ion complexes in aqueous solutions were investigated by SANS and SAXS techniques so as to elucidate the microscopic origin of the reentrant sol–gel transition (sol I–gel I–sol II–gel II transition with C_{CR}). It was found that CR ions form clusters by themselves in an aqueous solution, giving rise to a Bragg peak at about q = 0.1 Å^{-1}. By addition of PVA, an additional peak (or shoulder) appears in the Kratky plot at about q = 0.02–0.04 Å^{-1}, which is due to the modulation of the chain conformation from that in a neutral polymer solution by complexation and/or gelation. The structures of the PVA–CR ion complexes in both sol and gel states were analyzed by employing the combination of the Lorentzian and Gaussian scattering functions. The curve fitting of the observed scattered intensity with the Gauss–Lorentz-type function indicates that the structure parameters are sensitive to the sol–gel (sol I to gel I) and gel–sol (gel I to sol II) transitions as an increase and decrease in ξ, respectively. However the structure factors

are insensitive to the successive transition, i.e., sol II to gel II, due to a strong electrostatic screening effect of the CR ions.

Acknowledgment. This work is partially supported by a Grant-in-Aid, Ministry of Education, Science, and Culture, Japan (Grant-in-Aid, Nos. 04805092, 05805080, and 06651053 to M.S.). This work was performed with the approval of the Photon Factory of the National Laboratory for High Energy Physics, Tsukuba, Japan (Proposal No. 93G245), and the Solid State Physics Laboratory, The University of Tokyo (Proposal No. 93-59) at the Japan Atomic Energy Research Institute, Tokai, Japan. The authors are grateful to Prof. K. Kajiwara, Department of Materials Engineering, Kyoto Institute of Technology, and Dr. M. Imai, Solid State Physics Laboratory, The University of Tokyo, for fruitful discussions.

References and Notes

(1) Tsuchida, E.; Nishide, H. *Adv. Polym. Sci.* **1977**, *24*, 1.
(2) Prud'homme, R. K.; Uhl, J. T.; Poinsalte, J. P.; Halverson, F. *Soc. Petrol. Eng. J.* **1983**, Oct, 804.
(3) Sakurada, I. *Polyvinyl Alcohol Fibers*; Marcel Dekker: New York, 1985.
(4) Ochiai, H.; Kurita, Y.; Murakami, I. *Makromol. Chem.* **1984**, *185*, 167.
(5) Sinton, S. *Macromolecules* **1987**, *20*, 2430.
(6) Pezron, E.; Leibler, L.; Ricard, A.; Audebert, R. *Macromolecules* **1988**, *21*, 1126.
(7) Leibler, L.; Pezron, E.; Pincus, P. A. *Polymer* **1988**, *29*, 1105.
(8) Shibayama, M.; Sato, M.; Kimura, Y.; Fujiwara, H.; Nomura, S. *Polymer* **1988**, *29*, 336.
(9) Shibayama, M.; Yoshizawa, H.; Kurokawa, H.; Nomura, S. *Polymer* **1988**, *29*, 336.
(10) Fujiwara, H.; Shibayama, M.; Chen, J.; Nomura, S. *J. Appl. Polym. Sci.* **1989**, *37*, 1403.
(11) Saito, S.; Okuyama, H. *Kolloid Z.* **1954**, *139*, 150.
(12) Kawakami, H.; Fujiwara, H.; Kinoshita, Y. Jpn. Pat. S47-40894, 1972.
(13) Shibayama, M.; Adachi, M.; Ikkai, F.; Kurokawa, H.; Sakurai, S.; Nomura, S. *Macromolecules* **1993**, *26*, 623.
(14) Shibayama, M.; Moriwaki, R.; Ikkai, F.; Nomura, S.; *Macromolecules* **1994**, *27*, 1738.
(15) Shibayama, M.; Moriwaki, R.; Ikkai, F.; Nomura, S. *Polymer*, in press.
(16) Kurokawa, H.; Shibayama, M.; Ishimaru, T.; Nomura, S. *Polymer* **1992**, *33*, 2182.
(17) Wu, W.; Shibayama, M.; Kurokawa, H.; Coyne, L. D.; Nomura, S.; Stein, r. S. *Macromolecules* **1990**, *23*, 2245.
(18) Kajiwara, K.; Kohjiya, S.; Shibayama, M.; Urakawa, H. In *Polymer Gels*; De Rossi, D.; Kajiwara, K., Osada, Y., Yamauchi, A., Eds.; Plenum: New York, 1991.
(19) Shibayama, M.; Kurokawa, H.; Nomura, S.; Muthukumar, M.; Stein, R. S.; Roy, S. *Polymer* **1992**, *33*, 2883.
(20) Bastide, J.; Boue, F.; Buzier, M. *Springer Proc. Phys.* **1989**, *42*, 48.
(21) Hecht, A. M.; Duplessix, R.; Geissler, E. *Macromolecules* **1985**, *18*, 2167.
(22) Mallam, S.; Horkay, F.; Hecht, A. Geissler, E. *Macromolecules* **1989**, *22*, 3356.
(23) Mallam, S.; Hecht, A. M.; Geissler, E. *J. Chem. Phys.* **1989**, *91*, 6447.
(24) Mallam, S.; Horkay, F.; Hechit, A. M.; Renie, A. R.; Geissler, E. *Macromolecules* **1991**, *24*, 543.
(25) (a) Horkay, F.; Hecht, A. M.; Mallam, S.; Geissler, E.; Renie, A. R. *Macromolecules* **1991**, *24*, 2896. (b) The definition of Ξ is different from those in refs 21–25. The definition in this paper was intended to stress the analogy to the Guinier function, $I(q) = I(0) \exp[-R_g^2 q^2/3]$, for a dilute system, where R_g is the radius of gyration of the scatterers.
(26) Cohen, Y.; Ramon, O.; Kopelman, I. J.; Mizrahi, S. *J. Polym. Sci.* **1992**, *30*, 1055.
(27) Shibayama, M.; Tanaka, T.; Han, C. C. *J. Chem. Phys.* **1992**, *97*, 6829.
(28) Shibayama, M.; Tanaka, T.; Han, C. C. *J. Chem. Phys.* **1992**, *97*, 6842.
(29) de Gennes, P. G. *Scaling Concepts in Polymer Physics*; Cornell University Press: Ithaca, NY, 1979.
(30) Ueki, Y.; Hiragi, Y.; Kataoka, M.; Inoko, Y.; Amemiya, Y.; Izumi, Y.; Tagawa, H.; Muroga, Y. *Biophys. Chem.* **1985**, *23*, 115.
(31) Jinnai, H.; Schwahn, D.; Imai, M. Unpublished results.
(32) Shibayama, M.; Kurokawa, H.; Nomura, S.; Roy, S.; Stein, R. S.; Wu, W. *Macromolecules* **1990**, *23*, 1438.
(33) Stauffer, D. *Introduction to Percolation Theory*; Taylor & Francis: London, 1985.
(34) Shibayama, M.; Ikkai, F.; Nomura, S. *Makromol. Chem., Macromol. Symp.*, submitted for publication.